Anal. Bioanal. Electrochem., Vol. 10, No. 10, 2018, 1247-1258

Analytical & Bioanalytical Electrochemistry

2018 by CEE
www.abechem.com

Full Paper

Study of Sodium Aluminate Concentration Influence on the Corrosion Behavior of Plasma Electrolytic Oxidation (PEO) Coatings on 6061 Al Alloy

Zahra Masoomi Loghman,* Arash Fattah-alhosseini and Seyed Omid Gashti

Department of Materials Engineering, Bu-Ali Sina University, Hamedan 65178-38695, Iran

*Corresponding Author, Tel.: +98 8138257400

E-Mail: zahra.masoomiloghman@gmail.com

Received: 10 June 2018 / Received in revised form: 9 September 2018 / Accepted: 10 September 2018 / Published online: 31 October 2018

Abstract- In this study, the surface of 6061 Al alloy sheets were treated by plasma electrolytic oxidation (PEO) process to obtain oxide coatings. The voltage-time curves shows that the breakdown potential decreases with increasing of electrolyte concentration. The effect of concentration of PEO electrolyte on the corrosion behavior of the coatings was investigated. To assess the corrosion behavior, the potentiodynamic polarization plots were achieved and electrochemical impedance spectroscopy (EIS) measurements were carried out. The results of these analyses indicated that by reducing the concentration of sodium aluminate in the electrolyte, the corrosion rate of the coatings on the 6061 Al alloy significantly decreased. Moreover, the variation of sodium aluminate concentration in the electrolyte, led to modification of morphology and micro porosity of the coatings and alteration of the responses in the voltage-time. The coating processed in the electrolyte which contained 10 g L^{-1} sodium aluminate exhibited the best corrosion resistance.

Keywords- Al alloy, Plasma electrolytic oxidation coating, Sodium silicate, Electrochemical impedance spectroscopy

1. INTRODUCTION

Al and its alloys are known as an important group of materials with industrial applications such as aerospace and automotive [1]. The 6061 Al alloy belongs to the series of 6xxx that

contains magnesium and silicon in its composition [2]. Apart from the low density, Al and its alloys have electrical and thermal conductivities and also suitable strength to weight ratio for manufacturing, but they show poor corrosion resistance [3,4]. Hence, in order to prevent destructive corrosion, an appropriate coating is needed in different applications. Many methods exist to create a coating on Al and its alloys. Methods like electroless plating, chemical/physical vapor deposition, plasma spray, traditional anodizing, etc. In coatings prepared by conventional anodizing, there is a notable amount of porosity. This is caused by the acid and/or base solutions generating lots of environmental pollution [5-7].

Plasma electrolytic oxidation (PEO), is a modern method for preparing ceramic coatings on the surface of light metal alloys such as Al and its alloys in aqueous electrolytes at a thickness of about 10-100 microns [7,8]. PEO is highly regarded because of the low costs, the environmental sustainability through the use of alkaline electrolyte, simple required equipment and finally, easy setup and possibility of acquiring good corrosion and wear resistant behavior. PEO technique is similar to the traditional anodizing but unlike anodizing that carries out at low voltage (about 10-50 V), PEO is practicable at higher quantities of the breakdown voltages of the primary oxide films (about 150-800 V). By exerting high voltage, the plasma micro-discharge phenomena occur and after that myriad sparks on the surface become visible. Owing to the positional thermal act of the sparks, ceramic coating contains oxides of base metal with intricate oxides of elements in the electrolyte [8-10]. While, the coating operation is performed at temperatures higher than 1000 ˚C, temperature of the metallic substrate is relatively low and retains its properties during the process [11]. Upon reaching to the breakdown voltage, a large number of micro-discharge appears on the surface. During the process, the number of sparks decreases, and their size gets larger. Materials due to high temperature (~10^3–10^4 K) and pressure (~10^2 MPa) move into the discharge channels quickly and melt. The products of oxide cool in touch with electrolyte and then freeze [5,12-14].

The electrolyte is an important factor for coating by PEO technique. The electrolyte composition has crucial effect on morphology, thickness, composition of phase and coating growth. Typically, inorganic polymers, silicates, aluminates, and phosphates in the process of coating are used as a basic component [8, 15-17]. About the coating applied on Al substrate, the main solutions used by researchers are silicates solutions, also there are a few reports of the aluminate electrolytes [18]. PEO coating includes a porous amorphous outer layer and an internal compact crystalline layer [19]. In this work, PEO coatings were formed on the 6061 Al alloy substrates using four different concentrations of sodium aluminate in the electrolyte. In this work, PEO coatings were formed on the 6061 Al alloy substrates using four different concentrations of sodium aluminate in the electrolyte. The corrosion properties, coating morphology and thickness of the coatings were evaluated.

2. EXPERIMENTAL PROCEDURES

Samples of 6061 Al alloy prepared in the dimensions of 20 mm×20 mm×2 mm, were polished with SiC papers (up to 2000 grit). After cleaning with distilled water, samples were immersed in electrolytes including 10, 12, 14, and 16 g L^{-1} $NaAlO_2$ as a modifying agent, 9 g L^{-1} $Na_2B_4O_7.10H_2O$ as a stabilizing agent, and 1 g L^{-1} NaOH as a conductive agent [8] at 30 ˚C. The conductivity of solutions was measured with D812 Weilheim instrument. The temperature was controlled by water cooling system. With plasma electrolytic oxidation under positive unipolar DC supply and constant current density of 15 A/dm^2, at 100 Hz frequency, samples were coated for 15 min in the stainless-steel container. After coating, the samples were washed with distilled water and dried with the stream of air.

Coating morphology and thickness of them were examined with JEOL JSM-840A scanning electron microscope and thickness of the coatings was measured by the cross-sectional images using of Digimiser software. Phase analysis was studied using Italstructures APD2000 diffractometer and CuKα radiation. The 2θ ranges from 20° to 90° with 0.05° step size. Corrosion of the coatings made in this study were evaluated by potentiodynamic polarization and EIS measurements using a three electrodes flat cell including Pt plate as the counter electrode and Ag/AgCl saturated in KCl as the reference electrode. All of measurements related to corrosion assessment were gained by the μAutolab Type III/FRA2 system correlated with NOVA 1.11 impedance software. The working electrodes were plunged in 3.5 wt. % NaCl solution for 60 min. All the electrochemical tests were performed at least three times.

3. RESULTS AND DISCUSSION

3.1. Voltage-time curve

The voltage-time curves of 6061 Al alloy during the application of 15 A dm^{-2} anodic current density at different $NaAlO_2$ concentrations are illustrated in Fig. 1. Two parts can be seen in the curves. In the first part, voltage increases linearly with the time while there are sparks on the sample surface. The voltage rate are decreased swiftly with the advent of tiny sparks. Therefore, it is named as breakdown voltage. After a few seconds, the other part of the curve starts. In this part, the sparking is steady-state, curves have linear behavior and curves slope are constant. Changes in the electrolyte concentration can lead to change in the slope of voltage-time curve. However, the effect of $NaAlO_2$ concentration on the slope of the curve is very low. The breakdown voltage is strongly affiliated on the concentration of electrolytes.

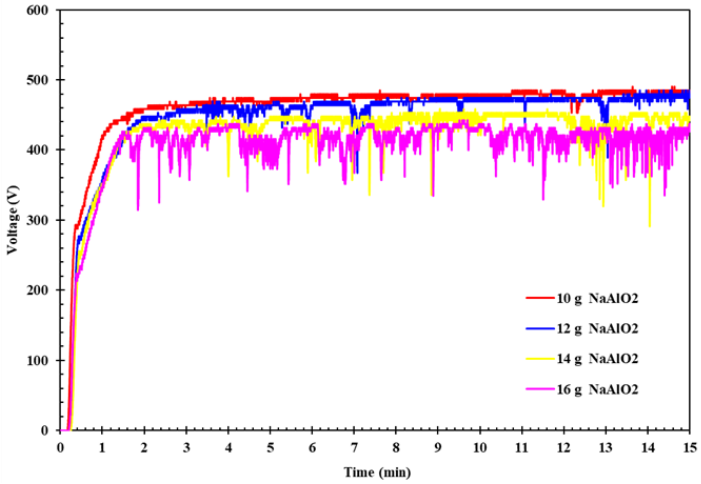

Fig. 1. Potential-time curves of PEO coatings on 6061 Al alloy in different concentration of $NaAlO_2$ at electrolytes

According to Fig. 1, with increasing of $NaAlO_2$ concentration, the slope of first part is decreased and breakdown potential is reduced. In the electrolyte containing 10 g L^{-1} $NaAlO_2$, the breakdown voltage is about 288 V. This value decreases to 272 V for 12 g L^{-1} $NaAlO_2$, 251 V for 14 g L^{-1} $NaAlO_2$, and 223 V for 16 g L^{-1} $NaAlO_2$. The conductivity of all electrolytes are presented in Fig. 2 and compared to sodium aluminate concentration. As it can be referred, with increasing of electrolyte concentration, the conductivity value increases and as a result we have a decreased break down potential. So dielectric breakdown occurs in lower voltage [20].

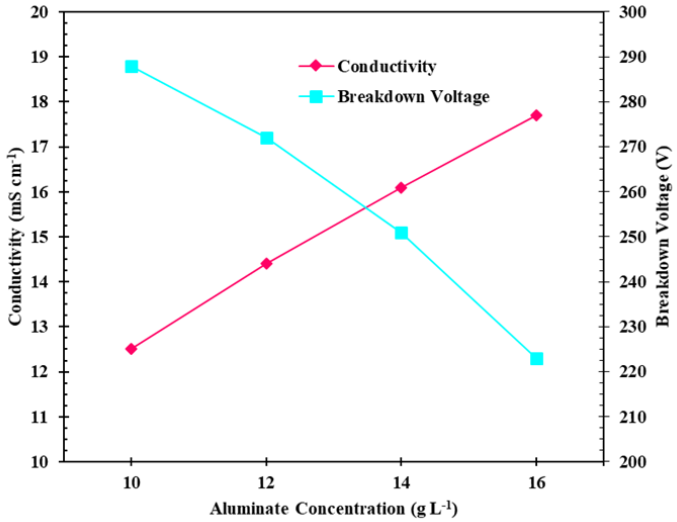

Fig. 2. Variations of conductivity and breakdown potential *vs*. concentration of sodium silicate at test electrolytes.

3.2. Morphology and microstructure of the coatings

Discharge characteristics and its changes during the PEO process, is crucial for evaluating the morphology of the coating [21]. Molten oxides and gas bubbles launched out of the discharge channel create the micro pores in the center of circular regions like the volcano crater are known as crater or pancake structures [22-26]. Micrograph of coated samples are illustrated in Fig 3. Concentration reduction of $NaAlO_2$, reduce the size of micro pores and their number. The micrograph for 16 g L-1 $NaAlO_2$ concentration shows a large amount of huge micro pores. It also presents that when the concentration of $NaAlO_2$ decreases, there are fewer and smaller micro pores. In 10 g L-1 $NaAlO_2$, the least micro pores in the structure exist. As it can be seen, all over the coating surface is covered by oxidizing materials with pancake-shaped morphology. The oxidizing materials around the discharge channels, which are related to a pancake formation, solidify quickly. This material around one discharge channel, solidifies once or in some cases, it may solidify repeatedly to make coating layers [13,27]. As it is shown in Fig. 3, the number of the pancakes has been increased with increasing the concentration of sodium aluminate in the electrolytes.

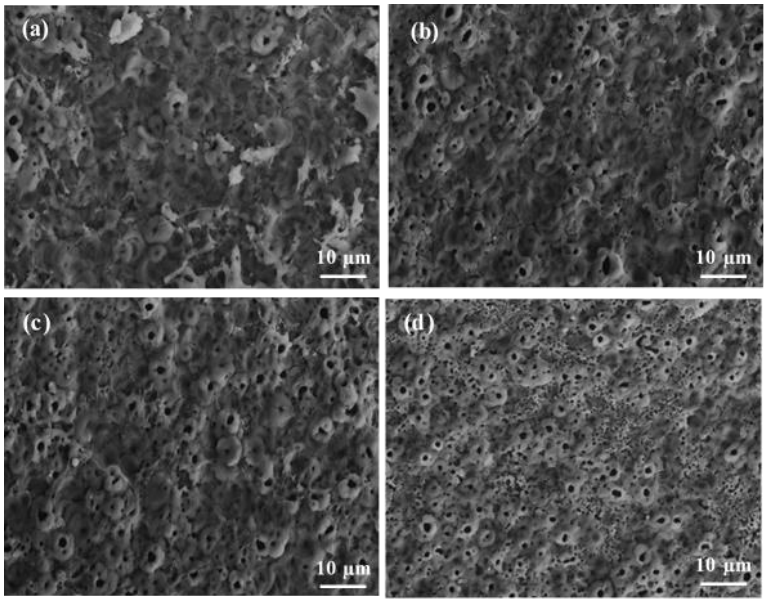

Fig. 3. SEM micrographs of 6061 Al alloy with PEO coatings: (a) 10 g L^{-1} $NaAlO_2$; (b) 12 g L^{-1} $NaAlO_2$; (c) 14 g L^{-1} $NaAlO_2$ and (d) 16 g L^{-1} $NaAlO_2$ at magnification of 1000x

Some micro cracks are formed in the boundaries of the pancake on the coating surface or around the pores due to the thermal stresses. Thermal stress can be made when the electrolyte with high cooling rate touches the coating layer during coating treatment [5,28-32].

3.3. Thickness of the coatings

In the cross section of the PEO coatings commonly three layers are observed. The "barrier layer" as an inner layer, locating in the vicinity of the substrate. Adjacent to the barrier layer, there is the "functional layer" with low porosity which covers about 70% of thickness of coating. In some samples, there is a third layer above the functional layer that is loose and porous [7,10,33]. The cross-sectional SEM images of the coatings formed in PEO electrolytes with different concentrations of sodium aluminate, are shown in Fig. 4. As it is illustrated, as the concentration of sodium aluminate in the electrolyte increased, the porosity in the coating increased. By reducing the amount of sodium aluminate to 10 g L^{-1}, the structure of the coating became smoother and the porosities were minimized. The coating created in the electrolyte containing 10 g L^{-1} of sodium aluminate is much denser and thicker compared to the coatings created in the electrolyte containing 12 and 14 g L^{-1} of sodium aluminate. Although the electrolyte contains 16 g L^{-1} of sodium aluminate creates a thicker coating but due to the porous structure, depending on natural differences and power of the sparks, the formed layer as a thicker coating is very lumpy and non-condense. In the other words, increasing the concentration of sodium aluminate can change the nature and power of sparks during the process. As it can be seen, the coating of 10 g L^{-1} sodium aluminate electrolyte, is highly integrated and smooth. With increasing the concentration of sodium aluminate in the electrolyte, porous and non-integrated coats are created.

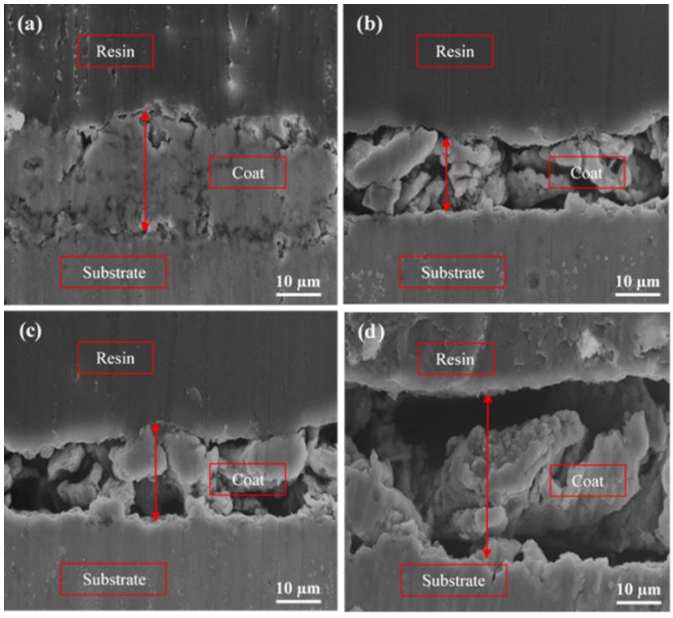

Fig. 4. Cross-section SEM micrographs of 6061 Al alloy with PEO coatings: (a) 10 g L^{-1} $NaAlO_2$; (b) 12 g L^{-1} $NaAlO_2$; (c) 14 g L^{-1} $NaAlO_2$ and (d) 16 g L^{-1} $NaAlO_2$ at magnification of 1000x

3.4. Composition of the coatings

Coating films on Al alloys mainly have α and γ alumina phases and contain two zones. A hard and dense zone of α-Al_2O_3 and a porous zone of γ-Al_2O_3 and other amorphous phases [34]. The remaining Mg, Cu and Zn ions in the coating is inversely proportional to the ratio of α to γ-Al_2O_3 [35]. α-Al_2O_3 is a stable phase with trigonal structure and melting point of 2050 ℃, while γ-Al_2O_3 is a meta-stable phase. The high cooling rates led to the formation of γ-Al_2O_3 and low cooling rates formed α-Al_2O_3 in the coating. In the early stages, a thin layer of alumina is formed. With rising up the temperature during coating process (T>1273 k), the metastable phase transforms to the stable phase. The dielectric breakdown occurs in the later stage of the PEO process in the energetic points [22,26,36]. X-ray diffraction pattern of substrate and coated samples are presented in Fig. 5. Al basic peaks are clear to detect. Also peaks of stable and metastable alumina phase are revealed. Due to the presence of Al metal in coating composition, the intensity of Al peaks in coating XRD spectra increased.

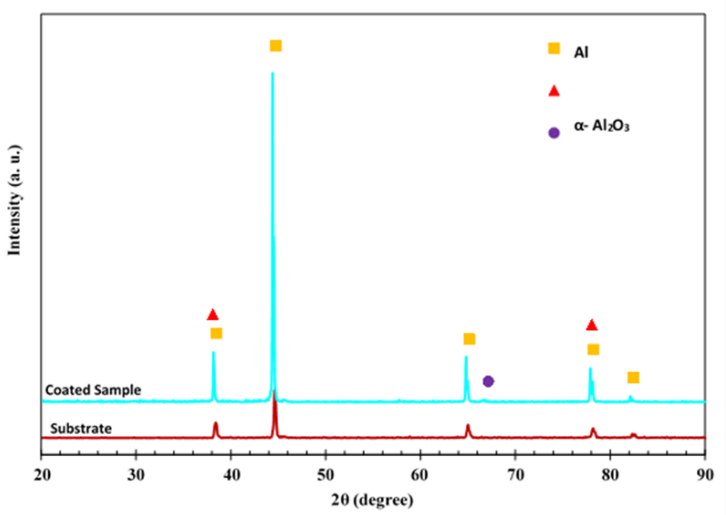

Fig. 5. X-ray diffraction patterns of 6061 Al alloy with and without PEO coating.

3.5. Corrosion behavior

3.5.1. Potentiodynamic polarization measurements

Potentiodynamic polarization plots of substrate and coated samples with different electrolyte concentration in 3.5 wt. % NaCl solution are illustrated in Fig. 6. As it is shown, the substrate has the highest corrosion current density and the most negative potential among all samples. The coated sample with 10 g L^{-1} sodium aluminate presents the best corrosion behavior.

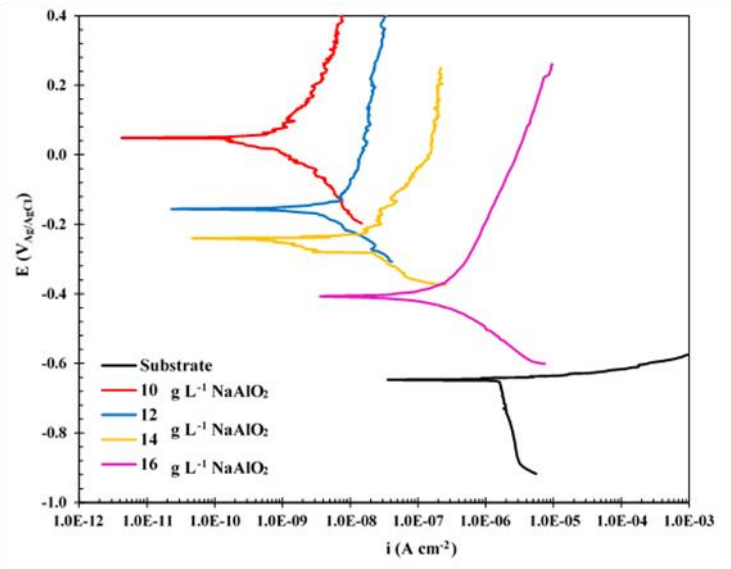

Fig. 6. Potentiodynamic polarization plots of PEO coatings on 6061 Al alloy in different concentration of $NaAlO_2$ at electrolytes.

In this case, the potentiodynamic polarization plot shifts to the left and up with applying coating process. Corrosion current density is about 6.9×10^{-10} A cm^{-2} and corrosion potential is +48 mV. These values are better than substrate and show the current density decrease of about four orders of magnitude. But with increasing the electrolyte concentration, the corrosion behavior gets worse. This behavior is in accordance with SEM micrographs shown in Figs. 3 and 4. The coating formed by 10 g L^{-1} electrolyte concentration, is denser and presents better protective behavior. On the other hand, the coating formed by 16 g L^{-1} electrolyte concentration, because of presence of high pores in its structure, have the higher corrosion current density (1.5×10^{-7} A cm^{-2}) and more negative corrosion potential (-405 mV) among all of the coated samples.

Table 1. Extracted data from polarization plots of substrate and coated samples

Sample	E_{corr} ($V_{Ag/AgCl}$)	i_{corr} (A cm^{-2})	E_p (%)
Substrate	-0.640	1.8×10^{-6}	------
10 g L^{-1} $NaAlO_2$	+0.048	6.9×10^{-10}	0.999
12 g L^{-1} $NaAlO_2$	-0.155	4.8×10^{-9}	0.997
14 g L^{-1} $NaAlO_2$	-0.238	1.2×10^{-8}	0.993
16 g L^{-1} $NaAlO_2$	-0.405	1.5×10^{-7}	0.916

With the increase of electrolyte concentration, corrosion current density of the coated samples increases about three orders and corrosion potential decreases 357 mV. Eq. (1) is using to measuring the inhibition efficiency (Ep %) [37]:

$$E_P\% = \frac{i^0_{corr} - i_{corr}}{i^0_{corr}} \times 100 \quad (1)$$

Where i_{corr} is the value of corrosion current density of PEO coatings and i^0_{corr} is the value of corrosion current density of substrate (6061 Al alloy). In Table 1 changes in the corrosion potential and variation of the corrosion current density and inhibition efficiency of all samples in 3.5 wt. % NaCl solution are presented.

3.5.2. EIS measurements

The EIS measurements by the Nyquist plots are presented in Fig. 7.

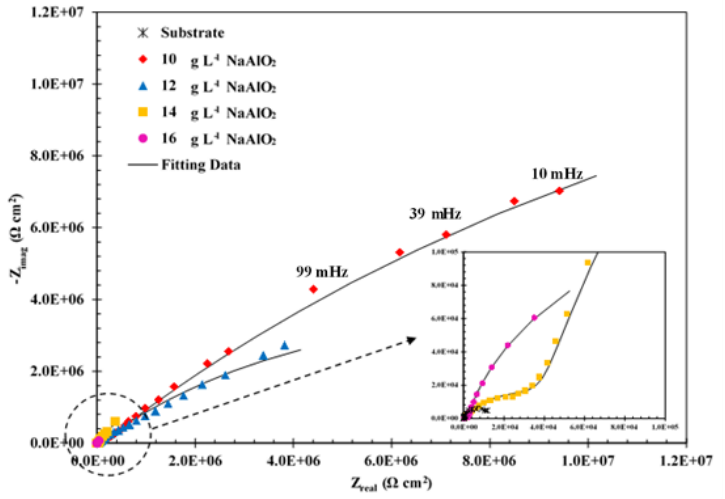

Fig. 7. Nyquist plots of PEO coatings on 6061 Al alloy in different concentration of $NaAlO_2$ in electrolytes

In these curves, the real impedance of each sample is plotted *vs*. the imaginary part of it at each frequency in 3.5 wt. % NaCl solution. As it is shown, the Nyquist plot of substrate made of one capacitive semicircle in the entire frequency regions representing a single time constant. This indicates the formation of electrical double layer on its surface. Using the electrical equivalent circuit (in Fig. 8), the measured impedance data of this specimen is simulated.

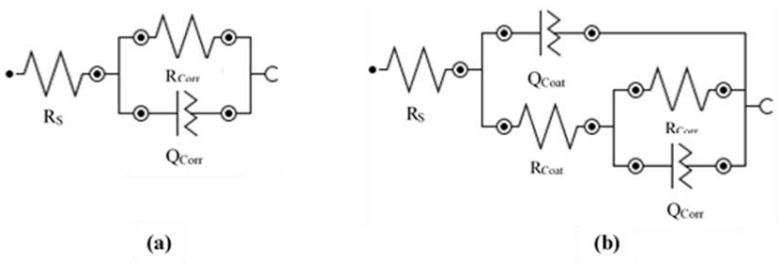

Fig. 8. Electrical equivalent circuits used to fit the impedance data of (a) substrate, and (b) PEO coating samples

In this circuit, the capacitive semicircle can be detected. R_s, R_{corr}, and Q_{corr} are the solution resistance, corrosion (polarization) resistance and constant phase element, respectively.

The diameter of semicircle is attributed to the corrosion resistance of the sample. The corrosion resistance of this substrate (6061 Al Alloy) in 3.5 wt. % NaCl solution is very low and it is necessary to apply a coating on its surface in order to improve the corrosion behavior. In this regard, Nyquist plots of 10, 12, 14, and 16 g L^{-1} sodium aluminate electrolyte concentration are illustrated in Fig. 7. In all of the coated samples two of capacitive semicircle have been appeared. The smaller semicircle is related to coating layer and the bigger semicircle can be attributed to electrical double layer of the metal surface. With increasing the electrolyte concentration, both of the mentioned semicircles become smaller and 10 g L^{-1} sodium aluminate electrolyte concentration presents the best corrosion behavior. In the equivalent electrical circuit given in Fig.8, R_{coat} and Q_{coat} are related to corrosion resistance and constant phase element of coating layer. The extracted resistance values for all of samples are presented in Table 2. The corrosion resistance of coating sample including 10 g L^{-1} sodium aluminate is 49300 kΩ cm^2 which is about 3600 times larger than the corrosion resistance of the substrate. In general, the penetration of NaCl solution in discharge channels determines the corrosion mechanism.

Table 2. Extracted data from electrical equivalent circuits of all Nyquist plots

Sample	R_{sol} (Ω cm^2)	R_{corr} (Ω cm^2)	Q_{corr}		R_{coat} (Ω cm^2)	Q_{coat}	
			Y_0 (Ω^{-1} s^{-n} cm^{-2})	n		Y_0 (Ω^{-1} s^{-n} cm^{-2})	n
Substrate	6.0±0.2	(1.3±0.2)×10^4	(1.0±0.1)×10^{-5}	0.912±0.02	---	---	---
10 g L^{-1} $NaAlO_2$	5.6±0.3	(4.9±0.4)×10^7	(2.5±0.2)×10^{-7}	0.490±0.02	(1.4±0.2)×10^5	(3.6±0.3)×10^{-9}	0.783±0.02
12 g L^{-1} $NaAlO_2$	5.8±0.2	(1.0±0.2)×10^7	(5.5±0.3)×10^{-7}	0.510±0.02	(5.4±0.4)×10^4	(2.7±0.3)×10^{-8}	0.645±0.02
14 g L^{-1} $NaAlO_2$	6.1±0.3	(1.8±0.2)×10^6	(8.1±0.4)×10^{-6}	0.864±0.02	(3.9±0.6)×10^4	(2.2±0.2)×10^{-6}	0.617±0.02
16 g L^{-1} $NaAlO_2$	5.9±0.2	(3.7±0.3)×10^5	(8.0±0.4)×10^{-5}	0.900±0.02	(2.6±0.2)×10^3	(1.3±0.1)×10^{-5}	0.510±0.02

4. CONCLUSION

The effect of sodium aluminate concentration in the PEO electrolyte on the corrosion behavior of PEOed coatings on 6061 Al alloy was studied in the present work. The PEO coatings on the surface of 6061 Al alloy were consisted of α and γ alumina. The thickness of coating in the electrolyte containing 10 g L^{-1} sodium aluminate, was about 30 μm and higher than the other coatings. Higher concentration of the sodium aluminate resulted in the electrolyte conductivity increase and consequently the breakdown voltage was decreased.

This reduction also diminished the corrosion resistance of the coating samples. The electrolyte containing 10 g L^{-1} sodium aluminate presented the best corrosion behavior. At this concentration, the corrosion resistance increased 3600 times in comparison with the bare substrate.

REFERENCES

[1] H. Fadaee, and M. Javidi, J. Alloys Compd. 604 (2014) 36.
[2] ASM Handbook Volume 2: Properties and Selection: Nonferrous Alloys and Special-Purpose Materials (1990).
[3] J. R. Davis, Corrosion of aluminum and aluminum alloys, ASM International, Materials Park (1999).
[4] M. Vakili-Azghandi, and A. Fattah-alhosseini, Metall. Mater. Trans. A 48 (2017) 4681.
[5] B. L. Jiang, and Y. M. Wang, Surface engineering of light alloys, Chapter 5, Plasma Electrolytic Oxidation Treatment of Aluminum and Titanium Alloys, H. Dong (Ed.), Cambridge UK: Woodhead Publishing Limited (2010).
[6] K. Funatani, Surf. Coat. Tech. 133 (2000) 264.
[7] F. C. Walsh, C. T. J. Low, R. J. K. Wood, K. T. Stevens, J. Archer, A. R. Poeton, and A. Ryder, Trans. Inst. Met. Finish. 87 (2009) 122.
[8] A. Fattah-alhosseini, M. Vakili-Azghandi, and M. K. Keshavarz. Acta Metall. Sin. (Engl. Lett.) 29 (2016) 274.
[9] A. Fattah-alhosseini, and M. Sabaghi Joni, J. Mater. Eng. Perform. 24 (2015) 3444.
[10] M. Vakili-Azghandi, A. Fattah-alhosseini, and M. K. Keshavarz, J. Mater. Eng. Perform. 25 (2016) 5302.
[11] S. Tsunekawa, Y. Aoki, and H. Habazaki, Surf. Coat. Tech. 205 (2011) 4732.
[12] J. A. Curran, and T. W. Clyne, Surf. Coat. Tech. 199 (2005) 168.
[13] J. H. Wang, M. H. Du, F. Z. Han, and J. Yang, Appl. Surf. Sci. 292 (2014) 658.
[14] X. Yu, L. Chen, H. Qin, M. Wu, and Z. Yan, Appl. Surf. Sci. 366 (2016) 432.
[15] M. Vakili-Azghandi, A. Fattah-alhosseini, and M. K. Keshavarz, Measurement 124 (2018) 252.
[16] A. Fattah-alhosseini, S. O. Gasht, and M. Molaie, J. Mater. Eng. Perform. 27 (2018) 825.
[17] A. L. Yerokin, V. V. Lyubimov, R. V. Ashitkov, Ceram. Int. 24 (1998) 1.
[18] Y. Cheng, J. Cao, M. Mao, Z. Peng, P. Skeldon, and G. E. Thompson, Surf. Coat. Tech. 269 (2015) 74.
[19] S. Moon, and Y. Jeong, Corros. Sci. 51 (2009) 1506.
[20] H. F. Guo, and M. Z. An, Appl. Surf. Sci. 246 (2005) 229.
[21] H. Deng, Z. Ma, X. Zhang, Y. Zhang, and X. Liu, Surf. Coat. Tech. 269 (2015) 108.
[22] M. Kaseem, M. P. Kamil, J. H. Kwon, and Y. G. Ko, Surf. Coat. Tech. 283 (2015) 268.

[23] X. Shen, X. Nie, H. Hu, and J. Tjong, Surf. Coat. Tech. 207 (2012) 96.
[24] R. O. Hussein, X. Nie, and D. O. Northwood, J. Alloys Compd. 541 (2012) 41.
[25] J. M. Wheeler, J. A. Curran, and S. Shrestha, Surf. Coat. Tech. 207 (2012) 480.
[26] Y. Chen, T. Cheng, and X. Nie, J. Alloys Compd. 578 (2013) 336.
[27] R. O. Hussein, X. Nie, D. O. Northwood, A. Yerokhin, and A. Matthews, J. Phys. D. Appl. Phys. 43 (2010) 105203.
[28] H. Duan, K. Du, C. Yan, and F. Wang, Electrochim. Acta 51 (2006) 2898.
[29] X. G. Han, X. P. Zhu, and M. K. Lei, Surf. Coat. Tech. 206 (2011) 874.
[30] W. Mu, and Y. Han, Surf. Coat. Tech. 202 (2008) 4278.
[31] W. Xue, Z. Deng, R. Chen, and T. Zhang, Thin Solid Films 372 (2000) 114.
[32] J. A. Curran, and T. W. Clyne, Acta Mater. 54 (2006) 1985.
[33] A. L. Yerokhin, A. Shatrov, V. Samsonov, P. Shashkov, A. Pilkington, and A. Leyland, Surf. Coat. Tech. 199 (2005) 150.
[34] S. V. Gnedenkova, O. A. Khrisanfovaa, A. G. Zavidnayaa, S. L. Sinebrukhova, P. S. Gordienkoa, S. Iwatsubob, and A. Matsuib, Surf. Coat. Tech. 145(2001) 146.
[35] Y. J. Guan, Y. Xia, and G. Lia, Surf. Coat. Tech. 202 (2008) 4602.
[36] T. Wei, F. Yan, and J. Tian, J. Alloys Compd. 389 (2005) 169.
[37] E. McCafferty, Corros. Sci. 47 (2005) 3202.